NASA Technical Paper 1754

Surface Pyrometry in Presence of Radiation From Other Sources With Application to Turbine-Blade Temperature Measurement

Donald R. Buchele

NOVEMBER 1980

NASA

NASA Technical Paper 1754

Surface Pyrometry in Presence of Radiation From Other Sources With Application to Turbine-Blade Temperature Measurement

Donald R. Buchele
Lewis Research Center
Cleveland, Ohio

National Aeronautics
and Space Administration

**Scientific and Technical
Information Branch**

1980

Summary

Surface pyrometry can be used to measure surface-temperature distributions on rotating turbine blades in jet engines. However, advanced turbofan engines, operating at high gas temperatures and pressures, can produce interfering gas radiation greater than the radiation from turbine blades. To measure and correct for interfering radiation, several methods were compared that use multiple-wavelength pyrometry. The methods included blade temperature reduction by increased blade cooling and use of one reference thermocouple on the blade. It was concluded from an error analysis of each method that measurement at two wavelengths was best for blade temperature determination. Accuracy of the measured temperature could be substantially improved by an auxiliary measurement, at the same two wavelengths, in which the pyrometer was sighted on a portion of the blade to which a thermocouple was attached. The conclusions are of general applicability to surface temperature measurement and not just to turbine-blade temperature measurement.

Introduction

Surface-temperature determination by measurement of the radiant energy emitted from the surface may be subject to errors caused by the presence of interfering radiation. A typical application in which this problem arises is the measurement of temperature distribution over the surface of a cooled turbine blade in a jet engine (ref. 1). Although the methods treated in this report are applicable to the general problem of surface-temperature measurement, the treatment will be directed specifically to the measurement of turbine-blade temperature because this measurement is of immediate concern (refs. 2 and 3) and because such specificity permits a quantitative estimate of attainable accuracy.

Tests have shown that thermal radiation emitted by turbine blades is augmented by radiation from gas, flame, or particulates in the line of sight of a pyrometer or by reflection of this radiation by the blades into the line of sight. This interfering radiation causes an error in blade temperature measurement. The magnitude of the error depends on blade temperature, blade emittance, gas temperature, and gas emittance. Correction for interfering radiation in other applications is considered in references 4 to 7. In application to a jet engine (as reported in ref. 1) radiance measurements at two wavelengths were used to determine blade temperature and effective gas emittance, with independently determined blade emittance and gas temperature.

In this report methods are considered that depend less on independently determined parameters. An error analysis of the methods enables their comparison. The results of the comparison provide a selection of methods that should lead to minimal error in blade temperature determination.

Analysis

Definition of Radiation Parameters

A pyrometer, sighted on a turbine blade in an engine, can receive blade radiation plus interfering radiation that is reflected by the blade from other sources. These sources include the surrounding blades, gas, flame, or particulates. The gas and the particulates in it are usually at a much higher temperature than is the blade itself. The radiation going from the blade to the pyrometer can be partially absorbed by the gas and by the particulates and supplemented by emission from the gas and the particulates. Considering all these sources of radiation, reflection, and absorption, it is reasonable to separate the observed radiation into two components: one from a source at a relatively low temperature that represents the blade radiation, and one from a source at a relatively high temperature that represents the effect of the gas and particulate radiation. The radiation originating from the blades can be represented by two parameters: a temperature T_b, and an effective emittance $\epsilon_{\lambda,b}$. The radiation originating from the gas (including flame and particulates) can be represented by two parameters, an effective temperature T_g and an effective emittance $\epsilon_{\lambda,g}$. (All symbols are defined in appendix A.) The radiation received by the pyrometer has a spectral radiance L_λ given by the sum of the two component radiances

$$L_\lambda = L_{\lambda,b} + L_{\lambda,g} \tag{1}$$

For error analysis the Planck radiation equation can be replaced by the Wien approximation. When the Wien equation is used, equation (1) becomes

$$L_\lambda = c_1 \lambda^{-5} \left[\epsilon_{\lambda,b} e^{-c_2/\lambda T_b} + \epsilon_{\lambda,g} e^{-c_2/\lambda T_g} \right] \quad (2)$$

The quantity $\epsilon_{\lambda,b}$ is an effective emittance that includes the effect of radiation from adjacent blades that is reflected from the blade under observation. The quantities T_g and $\epsilon_{\lambda,g}$ are an effective temperature and an effective emittance, respectively, that include the effects of gas or particulate radiation that is in the line of sight or that is reflected from the blade into the line of sight.

Radiation from the water vapor component of the gas and radiation from the turbine blade are compared in table I for a turbojet and for an advanced turbofan engine. Engine operating conditions are listed at the combustor, upstream and downstream of the first row of turbine blades, and at the turbine blade. The emittance of water vapor at 1 μm wavelength is calculated by using the gas absorption coefficient from reference 8. The product of ϵ_λ and the blackbody radiance L_λ at the listed temperature gives the radiance $\epsilon_\lambda L_\lambda$. The last column in table I is a ratio of gas radiance to blade radiance. With a 10-centimeter path length the gas radiance is comparable to the blade radiance for an advanced turbofan. Blackbody radiance is very large at the combustor temperature. Combustor radiation is shown in reference 1 to propagate downstream past the turbine inlet guide vanes and then to be reflected from the turbine blade at a level comparable to that of the blade radiation itself.

The computation of infrared radiant emission and absorption from 1 to 10 μm by combustion gases is extensively treated in reference 9. Because there is relatively little radiant emission from 0.6 to 1 μm, there is also a lack of published data on gas absorption constants in this band. Although the weakness of radiation in this region is an advantage for turbine-blade pyrometry, the lack of data prevents estimation of the gas spectral emittance. Actual measurement of the spectral emittance is required for each experimental situation. This stringent requirement can be simplified somewhat by eliminating the need to determine gas temperature and emittance as separate quantities. The two variables $\epsilon_{\lambda,g}$ and T_g in equation (2) can be replaced by $L_{\lambda,g}$ from equation (1) to give

TABLE I. - OPERATING CONDITIONS IN A TURBOJET AND AN ADVANCED TURBOFAN ENGINE

[Gas emittance estimated for H_2O at 1 μm; H_2O partial pressure, 0.13 of total pressure; viewing path length, 10 cm.]

	Static temperature, K	Total pressure, N/m^2	Emittance, ϵ_λ	Blackbody radiance, L_λ, W/cm^2 cm sr	Radiance, $\epsilon_\lambda L_\lambda$	Ratio of gas radiance to blade radiance, $\frac{(\epsilon_\lambda L_\lambda)_g}{(\epsilon_\lambda L_\lambda)_b}$
Turbojet:						
Combustor gas	2150	4.7×10^5	-------	153 000	-------	-----
Gas upstream of turbine blade	1150	4.7	0.0018	450	0.83	0.003
Gas downstream of turbine blade	920	1.7	.00077	22	.012	0
Turbine blade	1100	--------	1.0	260	260	-----
Advanced turbofan:						
Combustor gas	2590	37	-------	460 000	-------	-----
Gas upstream of turbine blade	2200	20	.0053	177 000	940	3.6
Gas downstream of turbine blade	1810	17	.0045	43 000	193	.7
Turbine blade	1100	--------	1.0	260	260	-----

$$L_\lambda = c_1 \lambda^{-5} \epsilon_{\lambda,b} e^{-c_2/\lambda T_b} + L_{\lambda,g} \quad (3)$$

For combustion gases where the emittance is much less than unity, gas radiances at two wavelengths, if once determined during a test, usually maintain the same radiance ratio $L_{2,g}/L_{1,g}$ to a higher degree than the absolute radiance at any one wavelength. For solid surfaces like those of turbine blades, the ratio of monochromatic emittances at two wavelengths and the same temperature are known or calculable with a higher percentage of accuracy than the absolute value of emittance itself. (When the emittance approaches unity as the upper limit because of the cavity effect of adjacent turbine blades, a ratio of reflectances at two wavelengths, that is, $(1-\epsilon_{2,b})/(1-\epsilon_{1,b})$, may be used instead of a ratio of emittances.) Consequently, where several equations of the form of equation (3) are to be solved simultaneously, the accuracy of the calculations is improved if the ratios are used in place of absolute values, as far as possible. This approach is tantamount to recognition that the quantities $L_{1,g}$, $L_{2,g}$, and $L_{3,g}$ are not truly independent variables but are related to each other. Similarly, the quantities $\epsilon_{1,b}$, $\epsilon_{2,b}$, and $\epsilon_{3,b}$ are not truly independent variables but are related to each other. The ratios $r_{i,b}$ and $R_{i,g}$ can be defined by the equations

$$r_{2,b} \equiv \epsilon_{2,b}/\epsilon_{1,b}$$

$$r_{3,b} \equiv \epsilon_{3,b}/\epsilon_{1,b}$$

$$R_{2,g} \equiv L_{2,g}/L_{1,g}$$

$$R_{3,g} \equiv L_{3,g}/L_{1,g}$$

Equation (3) written for three wavelengths thus becomes

$$\left.\begin{aligned} L_1 &= c_1 \lambda_1^{-5} \epsilon_{1,b} e^{-c_2/\lambda_1 T_b} + L_{1,g} \\ L_2 &= c_1 \lambda_2^{-5} \epsilon_{1,b} r_{2,b} e^{-c_2/\lambda_2 T_b} + L_{1,g} R_{2,g} \\ L_3 &= c_1 \lambda_3^{-5} \epsilon_{1,b} r_{3,b} e^{-c_2/\lambda_3 T_b} + L_{1,g} R_{3,g} \end{aligned}\right\} \quad (4)$$

Radiance is measured with an instrument having a bandpass spectral response. The error analysis assumes a sufficiently narrow bandpass for equations (4) to be defined for a monochromatic wavelength near the center of each pass band.

Table II lists values of the blade emittance ratios actually measured for some used blades taken from test engines. It must be emphasized that the ratios of effective emittances that appear in equations (4) are affected by blade surface deposits and the cavity effect of adjacent blades when blades are installed in an engine. These ratios are necessarily less well known than the ratios listed in table II, since these latter ratios were measured when the blade was isolated in a laboratory environment.

Radiometric Methods

In this discussion, we distinguish between the direct radiometric measurement obtained with the pyrometer and the independent determination of various parameters. The latter can be obtained by analytic computation, by a separate laboratory experiment, or by a measurement in situ with auxiliary instrumentation.

With a measurement of L_λ at one wavelength, equation (3) can be used to determine T_b when independent measurements are made of $\epsilon_{\lambda,b}$ and $L_{\lambda,g}$. The total error of T_b is caused by the error in radiometric measurements of L_λ and the error of each independent measurement. By virtue of equation (2) it is suggested that, when gas and blade

TABLE II. - EXAMPLES OF EMITTANCES AND EMITTANCE RATIOS

[Used blades measured at NASA, at 390 K blade temperature.]

Blade	Wavelength, λ, μm			Emittance ratio	
	$\lambda_1 = 1$	$\lambda_2 = 0.75$	$\lambda_3 = 0.55$	$\epsilon_{2,b}/\epsilon_{1,b}$	$\epsilon_{3,b}/\epsilon_{1,b}$
	Emittance, ϵ_λ				
B-1900	0.855	0.875	0.905	1.02	1.06
B-1900, later test	.91	.92	.93	1.01	1.02
Blade coated with $ZrSiO_4$ ceramic	.53	.555	.58	1.05	1.09

temperatures are different, measurement at two wavelengths would be effective in discriminating between blade and gas radiances in equation (1). Figure 1 shows blade and gas radiances in a spectral range from 0.55 to 1.0 μm, with typical temperatures T_b of 1100 K and T_g of 2000 K. The ratio $L_{\lambda,g}/L_{\lambda,b}$ of radiances substantially changes with wavelength. The blade radiance is a larger fraction of the total radiance at the longest wavelength; this wavelength is therefore most effective for determining blade emittance and temperature. At the shorter wavelength the gas radiance is a larger fraction of the total radiance; this wavelength is thus most effective in determining gas radiance. These conclusions about the relative effectiveness of the shorter and longer wavelengths assume that the gas spectral emittance is a constant value, such as that produced by particulates at the gas temperature. If the gas spectral emittance were to become 1/7 as great at 0.75 μm as it is at 1 μm (which is possible with gas molecular radiation), the equations at two wavelengths would become redundant, and their simultaneous solution would be indeterminate. Thus two wavelengths of measurement are not usable when the ratio $L_{\lambda,g}/L_{\lambda,b}$ of radiances is the same at both wavelengths.

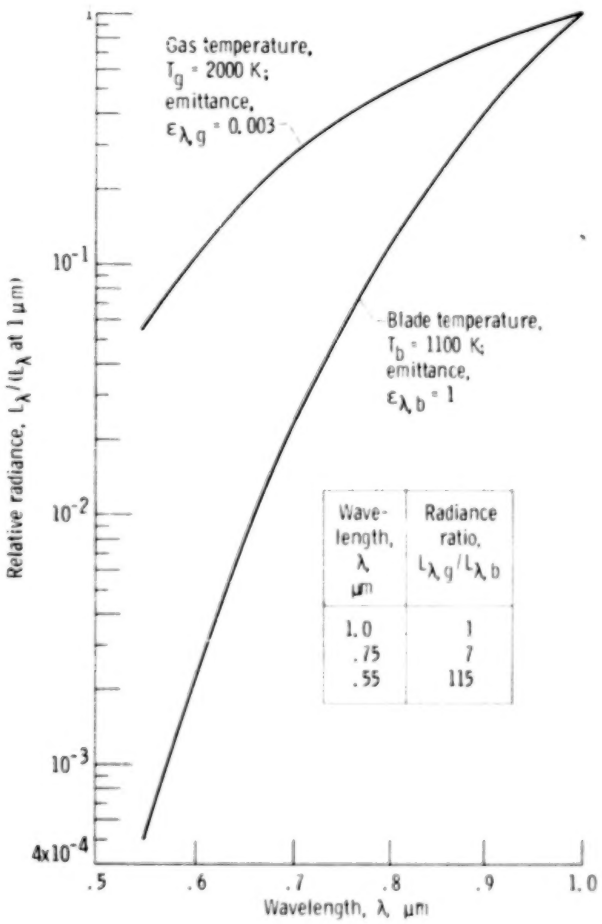

Figure 1. - Turbine blade and gas radiances.

The methods considered herein are those that may reduce the number of independently determined parameters or the degree of dependence of the temperature determination on those parameters. The methods are combinations of four different measurement conditions:

(1) Measurements at several wavelengths, A—Radiance measurements are made at two or three wavelengths. This method uses two independently determined parameters $\epsilon_{\lambda,b}$ and $L_{\lambda,g}$ at each wavelength, but only one radiance measurement is made at each wavelength.

(2) Measurements at two blade temperatures, B—increased blade cooling is used to produce a lower blade temperature with the same gas temperature. This method introduces one additional parameter, the second blade temperature T_b^* and an added radiance measurement L_λ^* at each wavelength.

(3) Thermocouple on the blade, C—A thermocouple is used to measure temperature at one point on the blade. The additional parameters $L_{\lambda,g}$ and $\epsilon_{\lambda,b}$ found when viewing the thermocouple junction can then be applied to determine blade temperature at other locations on the blade. The error in measuring temperature with the thermocouple is assumed to be negligible in comparison with the errors of optical pyrometry as here used.

(4) View a nonradiating surface, D—A low-temperature surface or a porthole is used to provide a surface with negligible radiation. Only gas radiation is measured. Since the line of sight does not intersect a blade, the gas radiation parameters may become different when the line of sight is directed at the blade during a test.

Some combinations of measurement conditions are listed in table III as methods 1 to 8. The column "Radiance measurements" lists the number of wavelengths and temperatures at which radiance measurements are made. The number of equations limits the number of parameters that can be solved for. The remaining parameters must be determined by independent, separately made measurements or estimates. When the number of equations exceeds the number of parameters to be solved for, a least-squares method of solution is to be used.

The methods are conveniently arranged in two groups. Primary methods are those that alone would suffice to determine T_b if there were adequate knowledge of the listed "Parameters to be independently determined." Auxiliary methods are those that are used in conjunction with one of the primary methods to provide an actual experimental determination of one or more of the parameters that must be independently determined, with resultant improvement in accuracy. The result of such combina-

TABLE III. - RADIOMETRIC METHODS

(a) Primary methods for determining blade temperature T_b

Method	Measurement conditions	Radiance measurements		Number of equations	Parameters solved for, P_j		Parameters independently determined, Q_k	
		Wavelength, L_λ	Temperature, K		Blade	Gas	Blade	Gas
1	A	λ_1	T_b	1	T_b	----------	$\epsilon_{1,b}$	$L_{1,g}$
2	A	λ_1, λ_2	T_b	2	T_b	$L_{1,g}$	$\epsilon_{1,b}, r_{2,b}$	$R_{2,g}$
3	A	$\lambda_1, \lambda_2, \lambda_3$	T_b	3	T_b	$L_{1,g}, R_{2,g}$	$\epsilon_{1,b}, r_{2,b}, r_{3,b}$	$R_{3,g}$
4a	A, B	λ_1, λ_2	T_b, T_b^*	4	T_b, T_b^*	$L_{1,g}$	$\epsilon_{1,b}, r_{2,b}$	$R_{2,g}$
4b	↓	λ_1, λ_2	T_b, T_b^*	4	T_b, T_b^*	$L_{1,g}, R_{2,g}$	$\epsilon_{1,b}, r_{2,b}$	----
5a		$\lambda_1, \lambda_2, \lambda_3$ λ_1, λ_2	T_b T_b^*	5	T_b, T_b^*	$L_{1,g}, R_{2,g}$	$\epsilon_{1,b}, r_{2,b}, r_{3,b}$	$R_{3,g}$
5b		$\lambda_1, \lambda_2, \lambda_3$ λ_1, λ_2	T_b T_b^*	5	T_b, T_b^*	$L_{1,g}, R_{2,g}, r_{3,g}$	$\epsilon_{1,b}, r_{2,b}, r_{3,b}$	----

(b) Auxiliary methods

6	A, C	λ	------	1	----------	$L_{\lambda,g}, R_{\lambda,g}$	$T_t, \epsilon_{\lambda,b}$	----
7	A, B, C	λ	T_b, T_b^*	2	$\epsilon_{\lambda,b}, r_{\lambda,b}$	$L_{\lambda,g}, R_{\lambda,g}$	T_t, T_t^*	----
8	A, D	λ	------	1	----------	$L_{\lambda,g}, R_{\lambda,g}$	----------	----

(c) Combinations of methods

2&6	A, C	λ_1, λ_2	T_b	4	T_b	$L_{1,g}, R_{2,g}$	$T_t, \epsilon_{1,b}, r_{2,b}$	----
2&7	A, B, C	λ_1, λ_2	T_b, T_b^*	6	$T_b, \epsilon_{1,b}, r_{2,b}$	$L_{1,g}, R_{2,g}$	T_t, T_t^*	----
2&8	A, D	λ_1, λ_2	T_b	4	T_b	$L_{1,g}, R_{2,g}$	$\epsilon_{1,b}, r_{2,b}$	----

tions with primary method 2 is listed in table III(c). Method 2 was selected as the best primary method. In some combinations of primary and auxiliary methods accuracy is further improved if the radiance measurements required for the auxiliary method are the same radiance measurements that were used in the primary method.

The methods of solution for T_b are

(1) Measurement at one wavelength, using one of equations (4)—The interfering radiation $L_{1,g}$ must be determined by an auxiliary method.

(2) Measurement at two wavelengths, using two of equations (4)

(3) Measurement at three wavelengths, using three of equations (4)

(4&5) Methods 2 and 3 repeated with additional measurements at a second, lower blade temperature—The methods differ in the number of parameters analytically determined. Methods 4b and 5b solve for all gas radiation parameters.

The auxiliary methods listed in table III(b) are one-wavelength measurements repeated at other wavelengths as needed. The methods are

(6) Measurement with a thermocouple on the blade, giving T_t at that point—This is an inverse of method 1, where T_b is solved for. When this method is applied at two or three wavelengths, the quantities $L_{\lambda,g}$ are expressed as ratios $R_{2,g}$ and $R_{3,g}$. Thus all independent gas parameters needed by methods 1 to 5 are determined. Some gain in accuracy may be expected by operating at minimum blade temperature in order to minimize blade radiation.

(7) Measurement with a thermocouple on the blade and with blade cooling to give two blade temperatures T_t and T_t^*—The use of two blade temperatures allows determination of blade emit-

tance; method 6 does not. Thus all independent parameters needed by methods 1 to 5 are determined. Where the conditions of the experiment permit, some gain in accuracy can be expected by applying this method in two steps. By operating at a test condition with small gas radiation, the blade emittance is more accurately determined. Then, by operating at the normal test condition where gas radiation is larger, $L_{\lambda,g}$ is more accurately determined.

(8) Measurement along a line of sight to a surface of negligible thermal radiation and negligible reflection of incident radiation—This method determines gas radiation along the line of sight, but it neglects gas radiation that may be reflected from the blade when the blade is viewed by methods 1 to 6. Thus the ratios $R_{2,g}$ and $R_{3,g}$ may be inaccurate when reflected gas radiation is significant.

The combinations of methods listed in table III(c), when compared with the primary method 2, show a transfer of some parameters from the column "Parameters independently determined" to the column "Parameters solved for." The resulting improvement in the accuracy of determining T_b is later derived by the error analysis and calculated for a specific example.

Error Estimate for Radiation Parameters

In the following discussion, an error of known algebraic sign in a variable x is denoted by dx, and a random error in x is denoted by δx.

The parameters solved for in table III have errors caused by

(1) The error of radiance measurement at each wavelength (type 1 error)

(2) The error of the parameters independently determined in table III (type 2 error)

In order to compute the errors by using matrices, let P_j represent parameters solved for, let Q_k represent parameters to be independently determined, and let L_i represent measured radiances at wavelengths λ_i.

Type 1 errors are derivable from

$$\left[\frac{dP_j}{P_j}\right]_1 = \sum_{i=1}^{n} W_{i,j}\left(\frac{dL_i}{L_i}\right)$$

$$\text{where } W_{i,j} = \left(\frac{\partial P_j}{\partial L_i}\right)\left(\frac{L_i}{P_j}\right) \qquad (5)$$

The quantity $W_{i,j}$ is called the error sensitivity coefficient. The nondimensional partial derivatives are obtained by inverting the matrix of nondimensional partial derivatives $(\partial L_i/P_j)(P_j/L_i)$. These derivatives are found with a computer program by numerically differentiating each equation for L_i with respect to the parameters P_j listed in table III for each method.

Methods 4a and 5a in table III have more equations than unknowns. The excess data are accommodated by an additional matrix manipulation that uses the least-squares method (ref. 10).

Type 2 errors are derivable from

$$\left[\frac{dP_j}{P_j}\right]_2 = \sum_{k=1}^{m} X_{j,k}\left(\frac{dQ_k}{Q_k}\right)$$

$$\text{where } X_{j,k} = \left(\frac{\partial P_j}{\partial Q_k}\right)\left(\frac{Q_k}{P_j}\right) \qquad (6)$$

The quantity $X_{j,k}$ can be expressed differently by noting that

$$\frac{\partial P_j}{\partial Q_k} = -\sum_{i=1}^{n}\left(\frac{\partial P_j}{\partial L_i}\right)\left(\frac{\partial L_i}{\partial Q_k}\right) \qquad (7)$$

where, under the summation sign, the first partial derivative is obtained from the solution of the simultaneous equations (4) but the second partial derivative is obtained from that one of equations (4) which represents L_i so that

$$X_{j,k} = -\sum_{i=1}^{n}\left(\frac{\partial P_j}{\partial L_i}\right)\left(\frac{\partial L_i}{\partial Q_k}\right)\left(\frac{Q_k}{L_i}\right) \qquad (8)$$

Many of the terms in equation (8) are zero in practice since, for example, the partial derivative of the radiance at the i^{th} wavelength with respect to the emittance at the k^{th} wavelength (i.e., $\partial L_i/\partial Q_k$, where $Q_k = \epsilon_{k,b}$) is zero.

The expression for the total random error in P_j due to random errors in both L_i and Q_k depends on whether any of the $Q_k (k = 1 \text{ to } l$, where $l < m)$ are determined by an auxiliary method that uses the same radiance measurements as the primary method. For such Q_k we note that

$$\frac{dQ_k}{Q_k} = \sum_{i=1}^{n} Y_{i,k}\left(\frac{dL_i}{L_i}\right) \qquad (k = 1,2,\ldots,l) \qquad (9)$$

where

$$Y_{i,k} = \frac{\partial Q_k}{\partial L_i}\,\frac{L_i}{Q_k} \qquad (10)$$

so that the total error is

$$\frac{dP_j}{P_j} = \sum_{i=1}^{n} W_{i,j}\left(\frac{dL_i}{L_i}\right) + \sum_{k=1}^{l}\left[X_{j,k}\sum_{i=1}^{n}(Y_{i,k})\left(\frac{dL_i}{L_i}\right)\right] + \sum_{k=l+1}^{m} X_{j,k}\left(\frac{dQ_k}{Q_k}\right)$$

$$= \sum_{i=1}^{n}\left[W_{i,j} + \sum_{k=1}^{l}(Y_{i,k}X_{j,k})\right]\frac{dL_i}{L_i} + \sum_{k=l+1}^{m} X_{j,k}\left(\frac{dQ_k}{Q_k}\right) \quad (11)$$

Then the total variance in P_j is given by

$$\left(\frac{\delta P_j}{P_j}\right)^2 = \sum_{i=1}^{n}\left[W_{i,j} + \sum_{k=1}^{l}(Y_{i,k}X_{j,k})\right]^2\left(\frac{\delta L_i}{L_i}\right)^2 + \sum_{k=l+1}^{m} X_{j,k}^2\left(\frac{\delta Q_k}{Q_k}\right)^2 \quad (12)$$

where $W_{i,j}$, $X_{j,k}$, and $Y_{i,k}$ are given by equations (5), (8), and (10), respectively.

Numerical Solutions and Selection of Methods

The nondimensional differential coefficients in equations (5) and (6) will be determined for a representative example where sources of error are sufficiently large to provide a clear indication of the relative merits of the various methods in securing accurate determination of T_b.

Assumed temperatures are 1100 K for the normally cooled blade, 1000 K for the blade when increased cooling is applied, and 2000 K for the gas. Assumed center wavelengths of measurement are 1, 0.75, and 0.55 μm; these are obtainable and measurable with bandpass filters and a silicon radiation detector. Subscript 1 applies to the longest wavelength, subscript 3 to the shortest.

Solutions for T_b by Methods 1 to 5

The error sensitivity coefficients for blade temperature are shown in figure 2 and table IV. In figure 2 the coefficient (eq. (5)) is caused by radiance measurement error; in table IV the coefficient (eq. (6)) is caused by an error of independently determined parameters. The abscissa $L_{1,g}/L_{1,b}$ in figure 2 is a ratio of gas radiance to blade radiance at 1 μm. The ratio includes the effects of blade and gas emittances. In table IV the error sensitivity coefficient for blade emittance is nearly independent of $L_{1,g}/L_{1,b}$, but the error sensitivity coefficient for gas radiance is nearly proportional to $L_{1,g}/L_{1,b}$. The total blade-temperature error indicated by each method is given by the square root of the sum of the squares of errors computed with the error sensitivity coefficients in figure 2 and table IV.

Solution for $\epsilon_{\lambda,b}$ and $L_{\lambda,g}$ by Methods 6 to 8

The error sensitivity coefficients for $\epsilon_{\lambda,b}$ and $L_{\lambda,g}$ are shown in figure 3 and table V, which parallel the previous figure 2 and table IV in definition of terms. As these methods are one-wavelength methods, the results are shown for each of the three wavelengths. In figure 3 the coefficient (eq. (5)) results from a radiance measurement error; in table V the coefficient (eq. (6)) results from an error in blade temperatures T_l and T_l^* as derived from thermocouple readings and

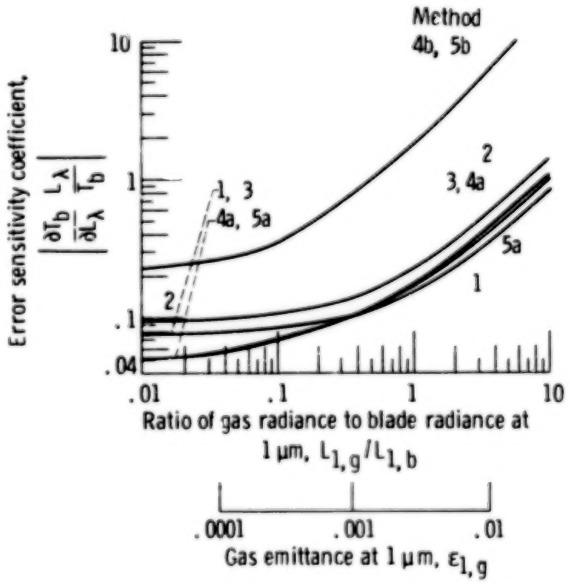

Figure 2. - Error sensitivity coefficients for methods 1 to 5. Temperature of blade with increased cooling T_b^*, 1000 K; temperature of cooled blade, T_b, 1100 K; gas temperature, 2000 K; blade emittance, $\epsilon_{\lambda,b}$, 1.

TABLE IV. - PRIMARY METHODS, ERROR SENSITIVITY COEFFICIENTS FOR BLADE TEMPERATURE CAUSED BY INDEPENDENTLY DETERMINED PARAMETERS WHEN $L_{1,g}/L_{1,b} = 1$

[Coefficients for gas radiance parameter are to be multiplied by actual $L_{1,g}/L_{1,b}$. Coefficients for blade emittance parameters are approximately independent of $L_{1,g}/L_{1,b}$.]

Method	Error sensitivity coefficients					
	$\frac{\partial T_b}{\partial \epsilon_{1,b}} \times \frac{\epsilon_{1,b}}{T_b}$	$\frac{\partial T_b}{\partial r_{2,b}} \times \frac{r_{2,b}}{T_b}$	$\frac{\partial T_b}{\partial r_{3,b}} \times \frac{r_{3,b}}{T_b}$	$\frac{\partial T_b}{\partial L_{1,g}} \times \frac{L_{1,g}}{T_b}$	$\frac{\partial T_b}{\partial R_{2,g}} \times \frac{R_{2,g}}{T_b}$	$\frac{\partial T_b}{\partial R_{3,g}} \times \frac{R_{3,g}}{T_b}$
1	-0.0768	(a)	(a)	0.0771	(a)	(a)
2	-.0808	0.0132	(a)	(a)	0.0948	(a)
3	-.0770	0	0.0006	↓	(a)	0.0784
4a	-.0776	-.0001	(a)		.0884	(a)
5a	-.0758	-.0029	.0006		(a)	.0764

[a]Quantity does not exist.

the estimated blade emittance $\epsilon_{\lambda,b}$. In table V the error sensitivity coefficients for gas radiance $I_{\lambda,g}$ are proportional to $1/(L_{1,g}/L_{1,b})$. The error sensitivity coefficients for blade emittance are independent of $L_{1,g}/L_{1,b}$. The total errors of $\epsilon_{\lambda,b}$ and $L_{\lambda,g}$ are given by the square roots of the sums of the squares of the errors computed with the sensitivity coefficients of table V and figure 3 when appropriate errors are assumed for $\bar{T}$, T^*, $\epsilon_{\lambda,b}$, L_λ, and L^*_λ.

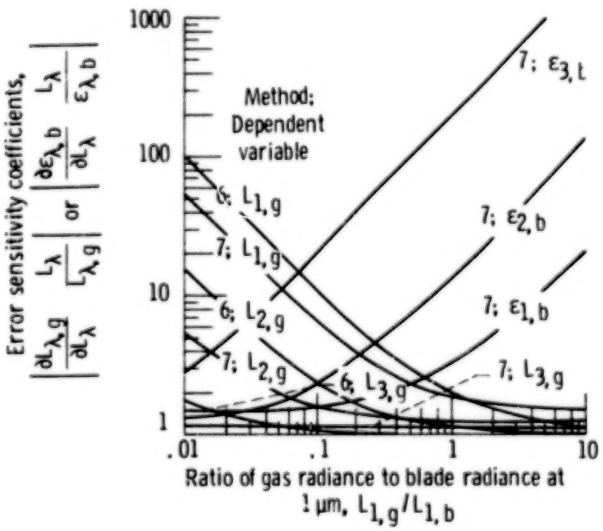

Figure 3. - Error sensitivity coefficients for auxiliary methods. Coefficient is 1.0 for method 8.

Selection of Radiometric Methods

Primary methods.—On the basis of figure 2 all methods except 4b and 5b appear equally acceptable because they yield comparable values for the error of radiance measurement. Narrower selection from the remaining methods can be attempted by using table IV and figure 3. Considering first the sensitivity to errors in gas radiance determination, there is no reason to prefer any one method because each coefficient listed in the last three columns of table IV (only one coefficient for any one method) has almost the same absolute magnitude. Figure 3 shows also that error sensitivity coefficients for all auxiliary methods are of comparable magnitude (between 1 and 2) whenever gas radiation is important ($L_{1,g}/L_{1,b} > 1$). Thus methods 1 to 5 are almost equally affected by any error of independently determined gas radiance.

In the absence of other strong reasons for choice among methods 1, 2, 3, 4a, and 5a on the basis of gas radiance, note that methods 2 to 5 yield a value for the absolute gas radiance $L_{1,g}$ and require independent determination only of a ratio $R_{2,g}$ or $R_{3,g}$, whereas method 1 requires independent determination of gas radiance. Thus methods 2 to 5 depend much less than method 1 on the accuracy of the data from the auxiliary methods. For this reason method 1 was eliminated.

Consider next the blade emittance. For each method listed in table IV the error sensitivity coefficient for blade emittance $\epsilon_{1,b}$ is substantially larger than the coefficients for $r_{2,b}$ and $r_{3,b}$. The coeffi-

TABLE V. - AUXILIARY METHODS, ERROR SENSITIVITY COEFFICIENTS CAUSED BY INDEPENDENTLY DETERMINED PARAMETERS WHEN $L_{1,g}/L_{1,b} = 1$

[When dependent variable is gas radiance, the coefficient is to be divided by the actual value of $L_{1,g}/L_{1,b}$. When dependent variable is emittance, the coefficient is independent of $L_{1,g}/L_{1,b}$.]

Method	Wavelength, λ, μm	Error sensitivity coefficient				
		$\frac{\partial L_{\lambda,g}}{\partial T_t} \times \frac{T_t}{L_{\lambda,g}}$	$\frac{\partial L^*_{\lambda,g}}{\partial T_t} \times \frac{T^*_t}{L^*_{\lambda,g}}$	$\frac{\partial L_{\lambda,b}}{\partial \epsilon_{\lambda,b}} \times \frac{\epsilon_{\lambda,b}}{L_{\lambda,g}}$	$\frac{\partial \epsilon_{\lambda,b}}{\partial T_t} \times \frac{T_t}{\epsilon_{\lambda,b}}$	$\frac{\partial \epsilon_{\lambda,b}}{\partial T^*_t} \times \frac{T^*_t}{\epsilon_{\lambda,b}}$
6	1.0	-13.0	(a)	-0.99	(a)	(a)
	.75	-2.43	(a)	-.14	(a)	(a)
	.55	-.19	(a)	-.01	(a)	(a)
7	1.0	4.8	-5.3	(a)	-17.9	5.3
	.75	.5	-.6	(a)	-21.1	4.1
	.55	.02	-.02	(a)	-26.2	2.7

[a]Quantity does not exist.

cients for $\epsilon_{1,b}$ are of similar magnitude for all methods listed. Thus methods 2 to 5 are equally affected by the error of the independently determined blade emittance.

In the absence of other strong reasons for selection among the methods, selection may be made on the basis of minimizing the number of measurements. Since method 2 requires the fewest number, it was selected.

Auxiliary methods.—It now remains to choose among method 2 alone and combinations of method 2 with one of the auxiliary methods 6, 7, and 8. Table VI lists the values of the error ratios that enter into the use of each of these method combinations, for four values of the ratio $L_{1,g}/L_{1,b}$. Table VI lists, in the second column, the square root of the sum of the squares of all the error coefficients that have radiance as an independent variable; this number represents the total error, in percent, caused by a 1 percent error in each radiance measurement. The remaining columns list the error coefficients for independently determined emittance parameters.

If the combination of methods 2 and 6 is used, the radiance measurements used in method 6 should be the same radiance measurements that were used in method 2. If this is done, errors due to an incorrect assumption of $\epsilon_{\lambda,b}$ cancel out; hence, an accurate determination of $\epsilon_{\lambda,b}$ is not necessary for the portion of the blade near the thermocouple. This statement is no longer fully accurate for regions of the blade where blade emittance is distinctly different from the emittance at the thermocouple. In such an event the cancellation of errors is not complete and a knowledge of the change in $\epsilon_{\lambda,b}$ is desirable to improve accuracy. This situation is not the situation treated in table VI.

Those combinations of methods where the variable under consideration is one of the variables solved for are indicated by footnote (a) in table VI.

When method 6 or 7 is used, any error in blade surface-temperature measurements with the thermocouple will introduce an equal error in blade temperature measurement. When method 8 is used, no error cancellation similar to that in method 6 occurs. However, because the gas radiance is measured, the error ratio $dT_b/dR_{2,g}$ is omitted, and the effects of radiance errors in determining $R_{2,g}$ are included in the error ratio dT_b/dL.

The coefficient values in table VI were calculated with the same ratio $L_{1,g}/L_{1,b}$ for both method 2 and the auxiliary methods. When these methods are applied sequentially, with different engine conditions, the ratio $L_{1,g}/L_{1,b}$ will be different for each method. This will change the values of the coefficients listed in table VI for the auxiliary methods. It is evident from figure 3 that smaller values of the coefficients will be obtained if $\epsilon_{\lambda,b}$ is determined by method 7 when $L_{1,g}/L_{1,b}$ is small and if $L_{\lambda,g}$ is determined by methods 6 or 7 when $L_{1,g}/L_{1,b}$ is large. Whenever possible this procedure should therefore be used.

Method 7 can be used for an initial determination of blade emittance, which is then used with method 6 for the majority of data taking. This procedure will reduce the time spent in cooling the blade.

TABLE VI. - TOTAL ERROR RATIOS FOR BLADE TEMPERATURE, WHEN DATA FOR METHOD 2 ARE SUPPLIED BY AN AUXILIARY METHOD

Radiance ratio, $\frac{L_{1,g}}{L_{1,b}}$	Total error ratio				
	$\frac{dT_b}{dL} \times \frac{L}{T_b}$	$\frac{dT_b}{dR_{2,g}} \times \frac{R_{2,g}}{T_b}$	$\frac{dT_b}{d\epsilon_{1,b}} \times \frac{\epsilon_{1,b}}{T_b}$	$\frac{dT_b}{dr_{2,b}} \times \frac{r_{2,b}}{T_b}$	$\frac{dT_b}{dT_t} \times \frac{T_t}{T_b}$
Method 2					
0.01	0.096	0.0009	-0.094	0.0132	(a)
.1	.106	.0094	↓	↓	↓
1	.217	.0948	↓	↓	↓
10	1.42	.9480	↓	↓	↓
Methods 2 and 6[b]					
0.01	0.135	(a)	0	0	1
.1	.150	↓	↓	↓	↓
1	.307	↓	↓	↓	↓
10	2.01	↓	↓	↓	↓
Methods 2 and 7[b]					
0.01	0.135	(a)	(a)	(a)	1
.1	.176	↓	↓	↓	↓
1	.354	↓	↓	↓	↓
10	2.29	↓	↓	↓	↓
Methods 2 and 8					
0.01	0.096	(a)	-0.094	0.0132	(a)
.1	.106	↓	↓	↓	↓
1	.255	↓	↓	↓	↓
10	1.95	↓	↓	↓	↓

[a]Quantity does not exist.

[b]Entries apply only where blade emittance is approximately equal to blade emittance near the thermocouple.

The accuracy of method 7 depends on the temperature difference $T_b - T_b^*$ produced by blade cooling. The effect of this temperature difference on the values of blade emittance error coefficients is shown in table VII for two values of the ratio $L_{1,g}/L_{1,b}$ and for λ_1, λ_2. Large values of the coefficients are found for blade emittance at λ_2 when $L_{1,g}/L_{1,b} = 1$. Small values are found when gas radiance is small, at $L_{1,g}/L_{1,b} = 0.1$. A temperature difference as small as 25 K can give acceptable accuracy.

The principal interest of this report has been maintenance of pyrometer accuracy in the presence of interfering gas radiation. This accuracy is always reduced by the presence of interfering radiation. It is thus important to demonstrate acceptable accuracy of the pyrometer under the ideal condition where there is no gas radiation. Accuracy of calibration and measurement is affected by the wavelength assigned to the bandpass filters. These topics are treated in appendix B.

TABLE VII. - ERROR SENSITIVITY COEFFICIENTS FOR AUXILIARY METHOD 7

[Coefficients are rms of coefficients at T_t and T_t^*.]

Error sensitivity coefficients	Radiance ratio, $\frac{L_{1,g}}{L_{1,b}}$	Wavelength, λ	Temperature difference between turbine blade and blade with increased cooling, $T_b - T_b^*$, K			
			25	50	100	200
$\left\lvert \frac{\partial \epsilon_{\lambda,b}}{\partial L_\lambda} \times \frac{L_\lambda}{\epsilon_{\lambda,b}} \right\rvert$	0.1	1	5.3	2.7	1.6	1.1
	.1	2	6.6	3.7	2.3	1.9
	1	1	59	33.1	20.7	15.8
	1	2	307	181	123	104
$\left\lvert \frac{\partial \epsilon_{\lambda,b}}{\partial T_t} \times \frac{T_t}{\epsilon_{\lambda,b}} \right\rvert$	0.1	1	62.4	32.3	18.7	13.9
	.1	2	63.3	33.9	21.5	17.8
	1	1	62.4	32.3	18.7	13.9
	2	2	63.3	33.9	21.5	17.8

Error Estimate for Blade Temperature

The error sensitivity coefficients that were presented in table VI for several methods are converted to blade temperature error by using assumed errors for radiance measurement and for blade and gas emittance parameters. The blade temperature error given by these methods is compared with the error of a one-wavelength pyrometer when gas radiation is ignored. (This is method 1 with an error $\delta L_{1,g} = L_{1,g}$.)

The blade temperature error is listed in table VIII for each assumed error, for four values of the ratio $L_{1,g}/L_{1,b}$. Table VIII lists, in the second column, the error caused by radiance measurement and, in the next four columns, the error caused by incorrectly estimating blade emittance and gas radiance. The last column is an rms total error of the preceding columns. The assumed errors listed in the column headings are obtained as follows:

(1) Radiance measurement error is $\delta L_\lambda / L_\lambda = 0.02$

(2) From table II, blade emittance $\epsilon_{1,b} = 0.91$, with error estimate $\delta\epsilon_{1,b} = 0.05$, gives $\delta\epsilon_{1,b}/\epsilon_{1,b} = 0.055$.

(3) From table II, the ratio $r_{2,b} = 1.01$, with error estimate $\delta r_{2,b} = 0.01$, gives $\delta r_{2,b}/r_{2,b} = 0.01$.

(4) For method 1 only, where $L_{1,g}$ is ignored, $\delta L_{1,g} = L_{1,g}$.

(5) The ratio $R_{2,g}$ depends on the emitter. For particulate matter the emittances at two wavelengths are nearly alike. For molecular emitters the emittances at two wavelengths may be substantially different. The ratio also depends on the gas temperature through the Wien equation, as shown by equation (1) and as plotted in figure 1 for the 2000 K gas. Because of the considerable variation in the ratio with engine operating conditions, an error $\delta R_{2,g}/R_{2,g} = 0.3$ is assumed.

Comparison of the rms total error for each method shows that method 2 is not better than method 1, for the assumed error $\delta R_{2,g}/R_{2,g}$. To show some improvement, it is necessary to determine $R_{2,g}$ with less than 30 percent error. The auxiliary methods are effective in doing this. Methods 2 and 6, and 2 and 7, also reduce the blade temperature error caused by blade emittance error. These methods also improve the accuracy when gas radiation is small.

Summary of Results

Several methods of using a multiple-wavelength pyrometer to measure interfering radiation have been shown by an error analysis to permit improvement in the accuracy of blade surface-temperature measurement. It was concluded that measurement at two wavelengths was best for blade temperature calculation. Accuracy of the calculated temperature was substantially improved by an auxiliary measurement at two wavelengths with the optical line of sight on an element of the blade surface where a thermocouple was attached to the blade. Blade emittance can also be determined by repeating the auxiliary

TABLE VIII. - COMPARISON OF BLADE TEMPERATURE ERROR BY SEVERAL METHODS USING ESTIMATED ERRORS OF RADIATION PARAMETERS

Radiance ratio, $\frac{L_{1,g}}{L_{1,b}}$	Temperature error of 1100 K blade					
	$\frac{\delta L_\lambda}{L_\lambda} = 0.02$	$\frac{\delta \epsilon_{1,b}}{\epsilon_{1,b}} = 0.055$	$\frac{\delta r_{2,b}}{r_{2,b}} = 0.01$	$\delta L_{1,g} = L_{1,g}$	$\frac{\delta R_{2,g}}{R_{2,g}} = 0.3$	rms total of all errors
Method 1 with gas radiation ignored						
0.01	0.17	4.6	(a)	0.8	(a)	4.7
.1	.19	↓	↓	8.0	↓	9.2
1	.34	↓	↓	61	↓	61
10	1.88	↓	↓	247	↓	247
Method 2						
0.01	0.21	5.7	0.15	(a)	0.31	5.7
.1	.23	↓	↓	↓	3.1	6.5
1	.48	↓	↓	↓	31	31.5
10	3.1	↓	↓	↓	310	310
Methods 2 and 6						
0.01	0.30	0	0	(a)	(a)	0.30
.1	.33	↓	↓	↓	↓	.33
1	.67	↓	↓	↓	↓	.67
10	4.4	↓	↓	↓	↓	4.4
Methods 2 and 7						
0.01	0.30	(a)	(a)	(a)	(a)	0.30
.1	.39	↓	↓	↓	↓	.39
1	.78	↓	↓	↓	↓	.78
10	5.0	↓	↓	↓	↓	5.0
Methods 2 and 8						
0.01	0.21	5.7	0.15	(a)	(a)	5.7
.1	.23	↓	↓	↓	↓	5.7
1	.56	↓	↓	↓	↓	5.7
10	4.3	↓	↓	↓	↓	7.1

[a]Quantity does not exist.

measurements after cooling the blade to obtain a temperature drop greater than 25 K. The methods discussed herein can be generalized to other applications of surface-temperature measurement in the presence of interfering radiation from other sources.

Lewis Research Center,
National Aeronautics and Space Administration,
Cleveland, Ohio April 15, 1980.
505-04.

Appendix A
Symbols

c_1	Planck's radiation constant, 3.7403×10^{-12} W cm^2
c_2	Planck's radiation constant, 1.4388 cm K
K	slope of line on graph
L	radiance
P	primary parameter to be solved for
Q	independently determined parameter
R	ratio of gas radiance at two wavelengths
r	ratio of blade emittance at two wavelengths
S	relative spectral response of detector
T	temperature
T_1	calibration temperature
V	measured voltage at temperature T
V_1	measured voltage at temperature T_1
W	error sensitivity coefficient, eq. (5)
X	error sensitivity coefficient, eq. (7)
Y	error sensitivity coefficient, eq. (10)
ϵ	emittance
λ	wavelength
τ	relative transmission factor of filter

Subscripts:

b	turbine blade
g	gas
T	temperature
T_1	calibration temperature
t	thermocouple
1,2,3	wavelengths (1, longest; 3, shortest)

Superscript:

*	turbine blade with increased cooling

Appendix B

Calibration and Computation Procedures

Calibration by Use of Effective Wavelength

The radiometer can be calibrated with a blackbody at two or more temperatures. The Wien function represents a linear relationship between the coordinates ln L_λ and $1/T$ when the wavelength is constant. Because of the bandwidth of the filter the wavelength to be used with the Wien function is not a constant but becomes shorter as the temperature rises. Thus a calibration curve in the form of a graph of ln L_λ as a function of $1/T$ is almost, but not fully, linear. The deviation from linearity will determine the number of calibration points required. Since the detector output voltage V is proportional to L_λ, ln V is also a nearly linear function of $1/T$. Thus linear interpolation can be used to give $1/T$ when ln V is known. The wavelength to be used with the Wien function at any temperature is derivable from the slope of the calibration curve and is given by

$$\frac{1}{\lambda} = -\frac{1}{c_2}\left[\frac{d \ln L_\lambda}{d(1/T)}\right] \tag{B1}$$

An alternative method, using a calibration at only one temperature T_1 as described in reference 11, is applied here to illustrate the concept and use of effective wavelength. The effective wavelength is an average wavelength that replaces the spectral passband of the pyrometer filter.

Typical examples of filter transmission and detector response are shown in figure 4. The filter bandwidths in this example are about 0.1 μm, about 10 percent of the average wavelength.

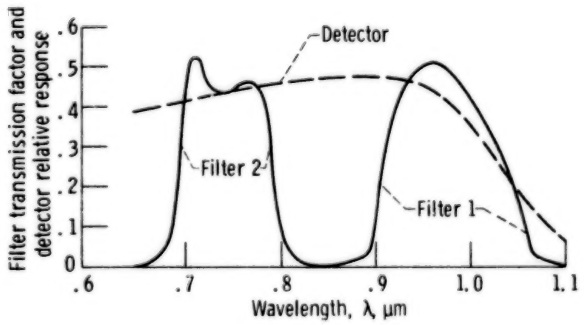

Figure 4. - Filter transmission factors and detector relative response.

The effective wavelength of a filter is dependent on temperature. The effective wavelength appears as λ_{T_1-T} when the radiance ratio $L_\lambda/L_{\lambda,1}$ or voltage ratio V/V_1 is written as

$$\frac{V}{V_1} = \frac{L_\lambda}{L_{\lambda,1}} = \exp\left[-\frac{c_2}{\lambda_{T_1-T}}\left(\frac{1}{T}-\frac{1}{T_1}\right)\right] \tag{B2}$$

where subscript 1 represents values at the calibration temperature and λ_{T_1-T} is the effective wavelength for the temperature interval T_1 to T. As the effective wavelength depends on T_1 and T, its defining equation will be derived. For a small interval where $T \simeq T_1$ the effective wavelength at T, designated λ_T, is a weighted average.

$$\frac{1}{\lambda_T} = \frac{\int_0^\infty (L_\lambda \tau S/\lambda)\mathrm{d}\lambda}{\int_0^\infty (L_\lambda \tau S)\mathrm{d}\lambda} \tag{B3}$$

where τ is the relative filter transmission factor and S is the detector relative spectral response. Only L_λ depends on T. The integration in equation (B3) is required for calibration, but it will be avoided for temperature computation. A graph of $1/\lambda_T$ as a function of $1/T$ is, to a good approximation, a straight line that has a slope K between the two temperatures T and T_1.

$$K = \frac{1/\lambda_T - 1/\lambda_{T_1}}{1/T - 1/T_1} \tag{B4}$$

Over the interval T to T_1, the average $1/\lambda$ gives the mean effective wavelength (ref. 11)

$$\frac{1}{\lambda_{T_1-T}} = \frac{1}{2}\left(\frac{1}{\lambda_{T_1}} + \frac{1}{\lambda_T}\right) \tag{B5}$$

Substituting equation (B4) in (B5) gives the mean effective wavelength independent of λ_T as

$$\frac{1}{\lambda_{T_1-T}} = \frac{1}{\lambda_{T_1}} + \frac{K}{2}\left(\frac{1}{T}-\frac{1}{T_1}\right) \tag{B6}$$

The slope constant K is calculated by using equation (B4) after equation (B3) has been numerically integrated by using filter and detector curves in figure 4 and the Wien function spectral radiance at the two temperatures T and T_1. The calibration will provide V_1 and T_1 for equation (B2).

To calculate an unknown temperature T, given the measured voltage V, equation (B2) is solved for T by using $\lambda_{T_1 - T}$ given by equation (B6) with an estimate of T. By one or two iterations between equations (B2) and (B6), the latest value of T is used with equation (B6) to get a better value for $\lambda_{T_1 - T}$, which gives a better value of T in equation (B2).

Experimental Check of the Calibration Procedure

The value of λ_{T_1} based on a calibration with a blackbody can be compared with a value calculated independently by integrating equation (B3). For example, the effective wavelength of the filters in figure 4, calculated with equation (B3) at $T_1 = 1190$ K gave the following result:

	Filter	
	1	2
λ_{T_1}, μm	0.977	0.756

An actual radiometer calibration with a blackbody at $T_1 = 1190$ K and one at $T_2 = 990$ K gave $\lambda_{T_1 - T}$ with equation (B2) and then λ_{T_1} with equation (B6). The results are

	Filter	
	1	2
V_1, volts	0.467	0.1629
V_2, volts	0.0381	0.00652
λ_{T_1}, μm	0.973	0.757
$\lambda_{T_1 - T}$, μm	0.975	0.759

The two methods show good agreement for λ_{T_1}. The disagreement for λ_{T_1} by the two methods is comparable to the difference between λ_{T_1} and $\lambda_{T_1 - T}$ for the temperature interval of 200 K.

The calibration data were also tested by computing the emittance of the blackbody with auxiliary method 7 in table III. The result is

	Filter	
	1	2
$\epsilon_{\lambda,b}$	0.988	0.989

References

1. Atkinson, W. H.; and Strange, R. R.: Pyrometer Temperature Measurements in the Presence of Reflected Radiation. ASME Paper 76-HT-74, Aug. 1976.
2. Uguccini, Orlando W.; and Pollack, Frank G.: High-Resolution Surface Temperature Measurements on Rotating Turbine Blades with an Infrared Pyrometer. NASA TN D-8213, 1976.
3. Atkinson, William H.; and Guenard, Robert N.: Turbine Pyrometry in Aircraft Engines. Electro/78 Conference Record. The Institute of Electrical and Electronics Engineers, Inc., 1978, Session 33/3.
4. Paul, Fred W.: Temperature Measurements with an Optical Pyrometer Under Adverse Conditions. Appl. Opt., vol. 3, no. 2, Feb. 1964, pp. 297-301.
5. Schilling, B. L.: Methods for Obtaining Surface Temperatures of Materials in the Presence of Extraneous Radiation. NASA TN D-4107, 1967.
6. Lowry, William P.; and Gay, Lloyd W.: Errors in Infrared Thermometry and Radiometry. J. Appl. Meteorol., vol. 9, Dec. 1970, pp. 929-932.
7. Einziger, R. E.; and Mundy, J. N.: Effect of Scattered Light on Temperature Measurement by Optical Pyrometry. Rev. Sci. Instrum., vol. 47, no. 12, Dec. 1976, pp. 1547-1550.
8. Ferriso, C. C.; Ludwig, C. B.; and Thomson, A. L.: Empirically Determined Infrared Absorption Coefficients of H_2 from 300 to 3000° K. J. Quant. Spectros. Radiat. Transfer, vol. 6, no.3, 1966, pp. 241-275.
9. Ludwig, C. B.; et al.: Handbook of Infrared Radiation from Combustion Gases. NASA SP-3080, 1973.
10. Feder, Donald P.: Automatic Optical Design, Appl. Opt., vol. 2, no. 12, Dec. 1963, pp. 1209-1226.
11. Kostkowski, H. J.; and Lee, R. D.: Theory and Methods of Optical Pyrometry. NBS-MONO-41, National Bureau of Standards, 1962.

1. Report No. NASA TP-1754	2. Government Accession No.	3. Recipient's Catalog No.
4. Title and Subtitle SURFACE PYROMETRY IN PRESENCE OF RADIATION FROM OTHER SOURCES WITH APPLICATION TO TURBINE-BLADE TEMPERATURE MEASUREMENT		5. Report Date November 1980 6. Performing Organization Code
7. Author(s) Donald R. Buchele		8. Performing Organization Report No. E-396
9. Performing Organization Name and Address National Aeronautics and Space Administration Lewis Research Center Cleveland, Ohio 44135		10. Work Unit No. 505-04 11. Contract or Grant No.
12. Sponsoring Agency Name and Address National Aeronautics and Space Administration Washington, D.C. 20546		13. Type of Report and Period Covered Technical Paper 14. Sponsoring Agency Code
15. Supplementary Notes		

16. Abstract

Surface pyrometry is feasible even when the amount of surface radiation is exceeded by radiation from surrounding sources. To measure and correct for this interfering radiation, several months that use multiple-wavelength pyrometry were compared by an error analysis. For a specific application to turbine-blade temperature measurement in a turbofan engine, it was concluded that a two-wavelength method was best and that auxiliary measurements at the same wavelengths could substantially improve the accuracy of the method.

17. Key Words (Suggested by Author(s))	18. Distribution Statement
Radiation pyrometry Turbine blades	Unclassified - unlimited STAR Category 07

19. Security Classif. (of this report)	20. Security Classif. (of this page)	21. No. of Pages	22. Price*
Unclassified	Unclassified	18	A02

* For sale by the National Technical Information Service, Springfield, Virginia 22161

NASA-Langley, 1980

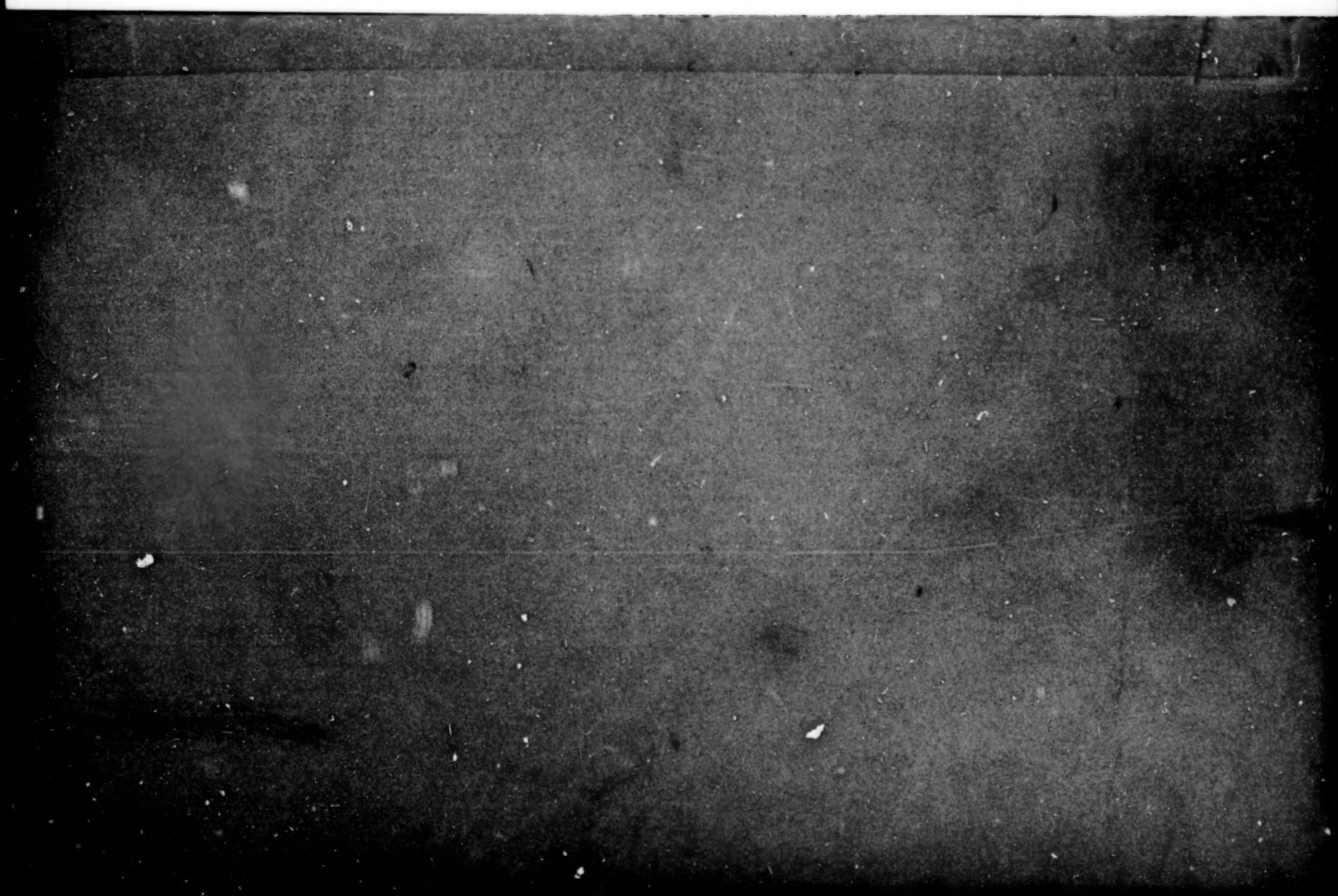

END

March 6, 1981